PERFORMANCE OF A HIGHWALL IN SOFT ROCK, HIGHVALE MINE, ALBERTA

C.A. Small[1] and N.R. Morgenstern[2]

[1] Engineer, Hardy BBT Ltd., 4810 - 93 Street, Edmonton, AB, T5J 2L4

[2] Professor, Dept. of Civil Engineering, University of Alberta, Edmonton, AB T6G 2G7

submitted

to

Canadian Geotechnical Journal

October, 1991

ABSTRACT

The Highvale Mine, west of Edmonton, Alberta is a strip mining operation with Upper Cretaceous soft sandstone and mudstone overlying the coal deposit. Highwalls cut in the soft rock experienced numerous failures from 1983 to 1985 that disrupted stripping and mining operations and posed a threat to safety.

The performance of a 20 to 23 metre highwall at Highvale was studied in 1987 and 1988 to gain insight to the mechanisms of failure. The study utilized surveying, slope indicators, and piezometers to determine the deformation and seepage pattern behind the highwall as it rebounded into the pit upon excavation. Translational movements were found to extend over 250 metres behind the highwall along weak, probably pre-sheared bentonitic mudstones. The sandstone and mudstone overburden was observed to extend toward the open pit. This affected the pore pressure regime and lead to a reduction in the mass strength of the sandstone and mudstone. The findings of this study contributed to a better understanding of the mechanisms of highwall failure in soft sedimentary rocks.

Keywords: highwall, deformations, failure, seepage, loosening, softening

1 Introduction

1.1 Objectives of Study

Failures of slopes in stiff clays and soft argillaceous rocks are difficult to understand because they are subjected to many processes. The materials are invariably fissured and therefore scale effects limit the value of laboratory testing to determine geotechnical properties. Pore pressure dissipation is often protracted in time and the materials are moisture sensitive leading to an additional reduction in strength with time due to softening. Significant differences between peak and residual strength indicate that the materials are also disposed to progressive failure. Moreover, in many instances the soil or rock has been acted upon in the past by geological processes that have induced slip planes that ultimately control stability. The ability to model numerically many of these processes often exceeds our understanding of them. Therefore, performance monitoring of slopes in stiff clays and soft rocks is a high priority activity if a clearer understanding of the influence of the various failure processes is to emerge.

This study evaluated the performance of an active mine highwall in soft rock to gain insight to the mechanisms contributing to failure. When a highwall is excavated and rebounds into the pit, the strength properties and pore pressures of the soil or rock behind the highwall can be affected. To understand how this ultimately affects stability, three objectives were specified:

1. Measure deformations in the rock behind the highwall and determine the resulting strains;
2. Measure the porewater pressures behind the highwall; and

3. Determine the zones of movement that could ultimately become slip planes during a failure

Previous comparable investigations (e.g. Burland et al, 1977; Esu et al, 1984) illustrate the value of such studies.

1.2 Highvale Mine

The study was conducted at the Highvale Coal Mine, because of numerous highwall failures that had occurred there from 1983 to 1985. Several workers had investigated these failures and reported on the geology of the area including: Moell et al (1984), Fenton et al (1986), Barron et al (1986), Wade and Peterson (1986), and Tsui (1988).

The Highvale Mine, shown in Figure 1, is located 80 km west of Edmonton, Alberta on the south shore of Wabamun Lake. TransAlta Utilities Corporation (TAU) operates Highvale which is one of the largest coal strip mining operations in Canada.

TAU kindly permitted the authors to perform the field investigation program in Pit 03 at Highvale. A description of the study site is provided in a subsequent section.

1.3 Mining Method

Figure 2 is a schematic of the strip mining procedure used at Highvale. Fifteen to 40 metres of till, sandstone, and mudstone overburden were removed by a dragline sidecast operation in strips 50 metres wide and several hundred metres long. The dragline was positioned on a bench that

was created during the previous cut. At the study site, the highwall was 20 to 23 metres high at an angle of 40° to 50°. The slope above the bench was 7 to 10 metres high at a 1H:1V slope.

With the overburden removed, electric shovels mined six horizontally bedded seams of coal. Each seam was from 0.50 to three metres thick, separated by thin partings of siltstone and mudstone, for a total thickness of 15 metres. The coal was mined so that the exposed face, or coalwall, was nearly vertical. The combined highwall and coalwall resulted in a rock slope 35 metres high at an average angle of 55° to 60°.

1.4 Bedrock Geology

Coal at Highvale was at depths of 15 to 40 metres, overlain by sand-, silt-, and mudstones of the Paskapoo Formation; Tertiary to Upper Cretaceous in age (Moell et al., 1984 and Fenton et al., 1986). The bedrock was cemented to uncemented with montmorillonite predominating the silt- and mudstones and with traces of montmorillonite in the sandstone. A 100 mm seam of bentonite rested just above the coal and was continuous throughout the study area. This thin seam was a major factor affecting the stability of the highwall, often acting as the basal shear plane for movements.

The coal was a non-marine, Upper Cretaceous and Paleocene rock, belonging to the Ardley Coal Zone which forms part of the Scollard Member (Moell et al., 1984). In general, the dip of the coal and overburden was less than 10 metres per kilometre in a westerly to southwesterly direction.

The overburden and coal was highly fractured, containing shear zones likely created by regional tectonic events, glacial tectonism, and permafrost, and further modified by weathering. Glacial tectonism, or ice thrusting, at Highvale has been investigated by several workers (Tsui, 1988 and Fenton et al., 1986) who have found dramatic evidence of bedrock blocks pushed by the glaciers, significantly damaging the material. This current study examined how the rock mass was further affected by rebound upon excavation.

1.5 Study Area, Pit 03

Figure 3 shows a plan view of the study site as it appeared in June, 1987 with six inclinometers (S1 to S6) and fourteen piezometers (P7 to P13, two per hole) installed. Figures 4 and 5 present north-south cross sections through each of the instrument lines. This site in Pit 03 was selected for the following reasons:

1. The highwall in Pit 03 had a history of instability with a number of past studies conducted there.
2. The geology at the study area was expected to be typical of several parts of the mine, such that the results from this study could be extended elsewhere at Highvale.
3. Mining would be active in Pit 03 with three new highwalls cut over the course of the study.
4. Site access was possible year round.

2 Stratigraphy

2.1 Sandstone

The soft sandstone was fine to medium grained with a number of hard cemented layers, the most prominent at elevations 727 and 740 metres. Some coal stringers and thin mudstone layers were also noted.

The sandstone was heavily jointed with near horizontal bedding. Three main joint sets were observed dipping near vertical and striking East Northeast, North Northwest, and East-West. These sets of joints were at spacings of 10 to 30 centimetres, creating sandstone 'blocks'. Some thin joints were infilled with 5 to 10 mm of clay while wider joints had a sand residue in them. More detailed joint surveys were not conducted since the sandstone blocks were small relative to the potential sliding masses. In addition it was difficult to discern which joints were due to blasting (to assist dragline excavation) and which ones were natural.

2.2 Sandstone/Mudstone Contact

The base of the sandstone was a distinct erosional surface cut into the mudstone. The sandstone/mudstone contact dipped about 0.5° to the south.

Evidence of glacial tectonic action was apparent along the contact on line S1-S3-S5 where geophysical logs showed a marked drop in density and the sonic logs indicated a crushed zone. This correlated well with previous findings (Moell et al, 1984) and it was conjectured that the contact may have been the basal shear plane of an ice thrust block. However, a similar trend was not found in holes S2-S4-S6.

2.3 Mudstone

Core samples and highwall mapping showed that the mudstone was heavily jointed in numerous directions. Other terms used to describe the mudstone were crushed, shattered, brecciated, and broken (Moell et al, 1984). Short, discontinuous slickensides were detected along many of the joint contacts.

The mudstone had several layers within it, varying in colours from blue-grey to brown with interbeds of carbon, clay clasts, siltstones, and coal. The plastic limit for this material ranged from 17 to 38 percent and the plasticity index was from 29 to 43 percent. Activities ranged from 0.58 to 0.97 confirming the presence of montmorillonite.

2.4 Bentonite

A 100 mm thick bentonite layer was located at the base of the mudstone, just above the main coal sequence (Figures 4 and 5). The bentonite layer was squeezed between two minor coal seams, 100 mm thick above and 300 mm thick below. The contact between the coal seams and the bentonite was wavy with amplitudes of less than one centimetre. The 300 mm thick coal seam was underlain by 400 mm of mudstone. A plastic limit of 51 percent and a platicity index of 95 percent was measured. The activity was about 1.2.

Shear planes had been observed within the bentonite and at the contact with the 100 mm thick coal layer above it at the highwall face. A similar observation was made from core that had been obtained from borehole S6

in June, 1987 when the highwall was 200 metres north of the borehole. Two slickensided surfaces were detected in the core: one was an undulating hairline crack within the sample and the other was at the contact with the upper coal layer.

Deformation observations since coring borehole S6 had shown that the excavation of the highwall did not trigger movements along the bentonite layer when the highwall was 200 metres away. Hence, the excavation could not have caused the slickensides that were found in the core and it was concluded that the bentonite layer was pre-sheared. Moreover, the shear planes were likely continuous for more than 200 metres, since they were observed simultaneously at the highwall face and in the core, 200 metres apart. When considering the stability of the highwall, it was assumed that the bentonite was at its residual strength.

2.5 Coal Sequence

One borehole, S3, was cored to beneath the 15 metre thick coal sequence for later installation of a deep inclinometer. From the core and examination of the coalwall, it was found that the partings that separated the economical coal seams consisted of siltstone and mudstone.

The parting between seams 4 and 5 was of particular concern because it was highly bentonitic. Face mapping detected three shear planes within it that were 2 to 5 cm apart and formed a shear zone.

Siltstone lay beneath the coal sequence.

3 Highwall Deformations

3.1 Inclinometers

Six vertical inclinometers (S1 to S6 in Figure 3) were installed on two lines, 50 metres apart, perpendicular to the highwall crest such that a pair of inclinometers was located on each of three cuts (21, 22, and 23). All of the inclinometers penetrated into the coal sequence but not below it.

3.2 Surveying

Surveying was used to locate the tops of each of the inclinometers in the TAU coordinate system. Surveying satisfied three objectives:

1. Provided redundancy to the monitoring scheme.
2. Permitted continued tracking of movements in the event that an inclinometer became 'pinched off' at depth.
3. Tracked movements of the inclinometers in relation to the mine coordinate system such that the absolute movement of the inclinometers was known. This was particularly important if the base of the inclinometer moved which was likely because none of the inclinometers penetrated below the coal sequence.

The surveys were conducted from two survey monuments well behind the highwall face, BM 1 and BM 2 in Figure 3. Details of the survey program are described by Small and Peterson (1988). Position accuracies of less than five millimetres were attained by using a one second theodolite, an electronic distance measuring device, a number of redundant readings, and least squares adjustment techniques. The location of the monuments were tied into the Trans-Alta Utilities mine coordinate system

to detect any movements that they may have experienced.

3.3 Mode of Deformations

The cumulative deflection profiles for inclinometers S2, S3, S5, andS6 are shown in Figures 6(a) to 9(a). The profile for inclinometer S1 was similar to the profiles for S3 and S5 and was not included in this paper for brevity. Likewise, S4 demonstrated a similar pattern as S2 and S6. The movements indicated in Figures 6(a) and 9(a) are northward, toward the pit. Eastward movements, parallel to the highwall, were less than 15 mm and were considered small enough to be neglected.

Figures 6(b) to 9(b) show the deflection over time at elevation 730 metres in the sandstone. One should note that the inclinometers have all been assigned an initial value of movement. This reflects the amount of movement that likely developed before the inclinometers were initialized on June 23, 1987.

Inclinometers S1 to S5 were tracked until they were excavated by the dragline, while S6 was monitored until it was 50 metres from the highwall crest. Of interest is the amount of movement that developed beneath inclinometers S1 to S6. Figures 6(a) to 9(a) indicate that even when the inclinometers were 50 metres from the highwall crest, their bases had moved 100 to 200 mm into the pit. The movements were likely along shear planes located beneath the inclinometers such as found in the mudstone parting between coal seams 4 and 5.

The pattern of movement differed between inclinometers S1, S3, and S5 and S2, S4, and S6. Two slip zones developed in the overburden along

line S1-S3-S5, one at the sandstone/mudstone contact and the second at the bentonite layer above the coal sequence. Along line S2-S4-S6, the highwall only moved at the bentonite layer, moreover the amount of total deformations was larger.

Figures 6(b) to 9(b) indicate that when the inclinometer was more than 50 metres from the highwall face, the movements stabilized in a matter of days after a highwall was cut. The same trend was apparent after the coalwall was excavated. Hence, it was concluded that beyond a distance of 50 metres from the highwall crest, the movements were essentially instantaneous.

When the inclinometer was within 50 metres of the highwall crest, the movements continued for some time after excavation of the highwall and coalwall. Immediately beneath the highwall crest, the movements tended to creep at rates of 1 to 3.5 mm/day, often continuing until when the next highwall was cut, 50 to 70 days later.

3.4 Deformation Field

The deformation field is defined in this instance as the variation in deformations in the overburden behind the highwall. For example, the deformations in the sandstone (at elevation 730 metres) for each of the inclinometers on February 15, 1988 are shown on Figure 10. Also included are the movements experienced by the benchmarks, BM1 and 2.

The arithmetic plot in Figure 10 was converted to a semi-log plot, Figure 11, which showed a striking linear relationship. The equation of the line can be represented by:

[1] $\text{Log } m = \text{Log } B + h\,M$

m = Movement toward the pit (northward direction);

B = Intercept of the straight line on the semi-log plot at a distance of zero, equivalent to movement at the highwall crest;

h = Horizontal distance behind the highwall crest;

M = Slope of semi-log line.

On Figure 11, a distinction was made between line S1-S3-S5 and line S2-S4-S6 because of the different deformation modes as discussed in the previous section.

Figure 12 presents the range of semi-log plots that were obtained over the course of the deformation monitoring program in 1987 and 1988. Note that the movements at the highwall crest ranged from 150 to 400 mm and extended for over 250 metres behind the highwall crest.

The same procedure was used to determine the deformation field in the

mudstone with the results shown in Small (1989). The results are not presented here because there is only a small difference in the amount of movements experienced by the sandstone and mudstone. Hence, the deformation field for the sandstone could be assumed to be representative of the overburden in general.

3.5 Lateral Strain Field

Given that the deformation field could be expressed as a function of horizontal distance from the highwall crest (Eqn. 1), then a strain distribution could be obtained by differentiating the deformation field over distance.

The expression for the lateral strain distribution becomes:

[2] $$\varepsilon_L = \ln 10 \cdot B \cdot M \cdot 10^{M \cdot h}$$

The strains calculated in this manner are horizontal or lateral strains. The calculated strains are negative indicating extension. For presentation here, the strains are plotted as positive values. The range of deformations shown in Figure 12 were recast to a range of lateral strains with the results shown in Figure 13. Figure 13 indicates that the sandstone experienced lateral, or extension strains, as high as 1.00 percent. At a distance of 250 metres behind the highwall face, the sandstone experienced strains of about 0.01 percent.

The extension of the overburden would have two components:

1. A volume expansion of the overburden material.
2. A spreading of the joints that were oriented more or less parallel to the highwall face.

When a highwall was excavated, the overburden would experience stress relief that would lead to a volume expansion of the sandstone and mudstone. Then as the coal was removed, the movement that was generated along slip planes below the overburden would cause the sandstone and mudstone joints to spread apart and hence lead to a loosening of the mass.

4 Piezometric Conditions

4.1 Piezometers

Two types of piezometers were used for this study: pneumatic piezometers installed in the low permeability mudstone and sealed open standpipes in the sandstone.

The pneumatic piezometer was a P100 tip supplied by SINCO. The sealed tip standpipe was a 50 mm (two inch) PVC pipe with a 10 foot slotted screen at the bottom. A bentonite seal was placed above and below the screen.

Two piezometers were installed in seven boreholes, P7 to P13, drilled with a solid stem auger adjacent to the inclinometer holes as shown in Figure 3. Figures 4 and 5 show the two piezometers in each hole, one at the bottom and the other at least two metres above it. Four holes had two pneumatic tips, while the remaining three had one pneumatic tip at the

bottom and a sealed tip standpipe above. The lower piezometer was identified with a "B" and the upper one with a "T".

4.2 Pore Pressure Response

Figure 14 presents typical outputs from two of the pneumatic piezometers located at the south side of the study site, P13-T and P12-B. They were initially installed 200 metres from the highwall crest and monitored as the highwall neared with successive cuts. Pore pressures at P13-T, in the sandstone, appeared to be solely a function of drainage. Piezometer P12-B, in the mudstone, also showed a drainage response until the highwall was 100 metres away. Then the pore pressures began to respond to stress relief during excavation. When the highwall was cut 50 metres away, the pore pressures in the mudstone dropped sharply and then recovered as a new steady seepage regime was established. A similar trend developed when the highwall was cut such that the crest passed near the piezometer.

4.3 Piezometric Model

To explore the impact of highwall rebound on the pore pressures, a piezometric model was prepared that summarized the pore pressure conditions in the overburden. The ultimate aim of this model was to see if the mechanism of joint spreading indicated by the deformation monitoring program had an impact on the groundwater flow regime.

Development of the model began by considering the piezometric heads 200 metres from the crest and establishing the flow conditions at that location. For example, Figure 14 shows that when P13-T was 200 metres

from the crest, a pressure head of 5.9 metres was measured and when P12-B was 200 metres away, the pressure head in the mudstone was 10 metres. These results were plotted on Figure 15. In addition, the results from the other piezometers along line S2-S4-S6 when they were 200 metres away from the crest were plotted.

For comparative purposes, a line with a slope representing the piezometric distribution for no vertical flow (i.e. hydrostatic condition) is shown on Figure 15. The actual position of the line on the plot has no physical significance. By comparing the slope of the actual piezometric distribution with the slope of the 'no vertical flow condition' line, it can be quickly deteremined if the groundwater seepate has a vertical flow component. A piezometric distribution with a steeper slope would indicate that there is a downward seepage component.

At 200 metres from the crest, the pressure heads in the sandstone indicated that there was no head loss in the vertical direction, that is, the flow was horizontal with no vertical component. The measurements in the lower part of the mudstone and upper coal also seemed to fall along a no vertical flow trend, however, the pressures were lower than in the sandstone. It is likely that an impervious layer existed at the top of the mudstone that perched the water in the sandstone and confined the water below it. Geophysical logging had indicated a zone of high density at elevation 727 metres which may have been the location of an impervious layer.

Figure 16 was prepared in a similar manner for a distance of 100 metres from the crest and also shows a perched water table in the sandstone and a confined aquifer in the lower mudstone and upper coal. Comparing Figures 15 and 16, the pressure heads decreased with proximity to the highwall

indicating horizontal flow to the face. In the lower sandstone, a deviation was beginning to develop from the hydrostatic condition.

At 50 metres from the highwall, Figure 17, the deviation noted in Figure 16 became extreme as shown. Flow in the lower sandstone had apparently changed from horizontal to vertical and the once impervious layer at the upper mudstone appeared to have breached.

The trends in Figure 17 were reinforced in Figure 18 which represents the pore pressure condition below the highwall crest one to two weeks after the highwall was cut. At that location, the predominant flow direction became vertical as water from the sandstone flowed through the mudstone into the coal.

The observations in Figures 15 to 20 led to the development of the piezometric model, Figure 21, a schematic of the groundwater flow pattern in the overburden. Between 50 and 100 metres from the highwall crest, the groundwater flow in the sandstone and mudstone changed from horizontal to vertical. The change in flow direction can be attributed to a breaching of an impervious layer at the upper mudstone as this layer strained laterally, causing once tight joints to spread apart and allowing water to flow through them.

5 Insight to Failure Mechanism

5.1 Failure Description

A small failure of the highwall in the spring of 1988 provided an opportunity to couple the performance observations with a failure mode.

The highwall failed in front of inclinometer S4 on Cut 21 in late March

and early April, 1988, Figure 20. On March 12, 1988, the dragline had completed overburden stripping at this location and the failure occurred one to four weeks after that time. It was contained in the highwall and did not extend into the bench.

The failure started in front of S4 and progressed over 100 metres eastward along the highwall. Figure 21 shows a cross section through the western end of the failed area with the geometry and stratigraphy before failure and the topography after failure. Two grabens had developed indicating that two distinct episodes of slip had occurred.

It was likely that the base of the failure was in the 100 mm thick bentonite seam located just above the coal sequence. Significant movements had been measured in this seam before failure and its location satisfied the post failure geometry.

The backscarps for the failures that were visible in the sandstone were inclined 80° to 85° to the horizontal. With the basal slip plane and a portion of the backscarp known, then the likely location of the complete slip surface was estimated as shown in Figures 21.

Based on the above observations, the failure was best described as an "earth block slide" in accordance with the classification put forth by Varnes (1978). Similar slides have occurred previously at the mine and other workers have termed this to be a composite failure combining a steep rotational slip plane at the backscarp with a near horizontal basal plane (Wade and Peterson 1986, Fenton et al. 1986, and Tsui 1988).

5.2 Pore Pressures and Strengths

Back analysis of the failure referred to the slip closest to the toe as the "toe failure" with the second slip called the "rear failure". Observations of the post failure area indicated that the toe failure took place likely one to three weeks after the highwall was cut (between March 18 and April 2, 1988) and the rear failure occurred three to four weeks after the cut was made (on approximately April 4, 1988).

It was fortunate that the failure occurred in front of the most instrumented section of the study site. The piezometer observations could then be utilized in the back analyses. The pore pressure trends presented in that section were extrapolated to the rear and toe failures by assuming a parabolic decrease in pressure head toward the toe. The piezometric records indicated that negative pore pressures were unlikely on the slip plane in the mudstone.

Figure 22 shows the assumed water pressure distribution at the toe one to two weeks after the highwall was cut. Figure 23 presents the piezometric head three to four weeks after the cut was made, applicable to the rear failure.

Failure in the sandstone was assumed to be partly controlled by the near vertical joint set that trended East-West, parallel to the highwall crest. Exposures of the near vertical slip planes at the backscarps of the toe and rear failure, were free of any clay and it was therefore assumed that the upper part of the slip plane travelled along a clean joint. Beneath the visible portion of the slip surface, it was assumed that failure took place along other joints and through blocks of intact sandstone.

Laboratory testing had indicated a peak friction angle of 44° and a residual angle of 40° for the sandstone. The joint that controlled the upper part of the failure was assigned residual strength parameters ϕ = 40° and c = 0 kPa. The remainder of the slip surface in the sandstone was expected to have a friction angle of about 40°. The cohesion was left unassigned and was to be determined by the back analysis.

For the mudstone, the scale of the failures was large enough compared to the small joint spacing to assume that the mudstone would behave in a homogeneous fashion. A friction angle of 22° was selected for the mudstone based on laboratory strength tests. The cohesion mobilized in conjunction with this friction angle was to be found by back analyses.

As indicated in Section 2.4, the bentonite was assumed to be presheared and residual strength parameters were applied in stability analyses. A residual angle of 12° was measured in the laboratory on samples near the presheared plane, however, experience with this material has found that the in-situ slip plane would likely have a lower strength. As a result, an angle of 10° was chosen as a the strength along the basal slip plane. The cohesion was set to zero.

5.3 Failure Back Analysis

Two dimensional, limit equilibrium stability analyses were used to determine the sandstone and mudstone cohesions mobilized at failure. Drained conditions were assumed throughout because the fissured nature of the materials would probably allow for adequate dissipation of excess pore pressures. The Morgenstern and Price method of stability analysis was

used with the computer program PC-SLOPE (Fredlund, 1985).

Figure 24 shows the results for the back analysis of the toe failure. It was found that for an assumed value of sandstone cohesion of 10 kPa, then a corresponding mudstone cohesion of 35 kPa was required to provide a Factor of Safety (FOS) of unity. During the analyses, when a sandstone cohesion of more than 20 kPa was assumed, then the force and moment equilibrium FOS would not converge and a solution was not possible. Hence, extrapolations beyond this value of sandstone cohesion are tentative.

Figure 25 shows the results from the back analysis of the rear failure overlain on the results from the toe failure. It is interesting to note that for any value of sandstone cohesion, then the mudstone cohesion decreased from the rear failure to the toe failure. The same can be said about the sandstone cohesion for any value of mudstone cohesion. It is possible that both the sandstone and mudstone cohesion simultaneously decreased from the rear to the toe. Hence, it can be concluded that the sandstone and mudstone strengths decreased with proximity to the highwall toe.

5.4 Failure Mechanism

The deformation observations and pore pressure model had demonstrated that the sandstone and mudstone experienced an expansion which lead to a separation of the joints. This would have loosened and softened the overburden, the latter resulting from water infiltrating newly opened cracks. The loosening mechanism would likely have affected the sandstone more so than the mudstone while the mudstone would have been more susceptible to softening.

As indicated by the lateral strain measurements, the lateral strains at the toe of the highwall were likely greater than at the location of the rear failure. The results of the failure analysis suggest that the strength of the overburden was inversely related to the lateral strains. With greater lateral strains, there would have been more loosening and softening of the rock mass.

6. Conclusions

The performance measurements obtained during this study were invaluable toward understanding the mechanisms of highwall failure at Highvale Mine. This study concluded the following:

1. The presheared bentonite was likely the basal slip plane for highwall failures and should be assigned residual strength parameters.
2. As the highwall rebounded into the pit, it underwent an expansion, measurable as a lateral strain, that affected the material strength and pore pressures in the following manner:
   a. The mass strength of the sandstone and mudstone was deteriorated by the spreading of the joints.
   b. As water flowed through the separating joints, there was an opportunity for softening to further reduce the mass strength of the sandstone and particularly the mudstone.
   c. As the groundwater flow changed from horizontal to vertical, very low pore water pressures developed below the highwall crest.
3. Lateral strain as high as 1percent developed near the face.

Acknowledgements

The authors wish to express their thanks to TransAlta Utilities for permitting this study to be conducted at Highvale. The superb cooperation of the TAU personnel was appreciated. Manalta Coal Limited also deserves recognition for their assistance. Financial support for this study was provided by the Alberta Office of Coal Research and Technology and the

Natural Sciences and Engineering Research Council of Canada.

References

Barron, K., Stimpson, B., and Kosar, K., 1986. A regressive mode of highwall failure in coal strip mines. Canadian Institute of Mining Bulletin. Vol. 79 (892), pp. 73-78.

Burland, J.B., Longworth, T.I. and Moore, J.F., 1977. A study of ground movement and progressive failure caused by a deep excavation in Oxford Clay. Geotechnique, Vol. 27, pp. 557-591.

Esu, F., Distefano, D., Guisolia, M. and Tancredi, G., 1984. Stability of a high cut in overconsolidated lacustrine deposits. Proc. 4th International symposium on Landslides, Toronto, Vol. 2, pp. 63-68.

Fenton, M.M., Trudell, M.R., Pawlowicz, J.G., Jones, C.E., Moran, S.R., and Nikols, D.J. 1986. Glaciotectonic Deformation and Geotechnical Stability in Open Pit Coal Mining. International Symposium on Geotechnical Stability in Surface Mining, Calgary, Alberta. pp 225-233.

Fredlund, D.G., 1985. PC-SLOPE Slope Stability Analysis, User's Manual S-30. Geo-Slope Programming Ltd., Calgary, Alberta.

Moell, C.E., Pawlowicz, J.G., Trudell, M.R., Fenton, M.M., Langenberg, C.W., Sterenberg, G.J., and Jones, C.E., 1984. Highwall Stability Project, Highvale Mine, Report of 1984 Activities. Alberta Research Council Report to TransAlta Utilities Corporation.

Small, C.A. 1989. Failure in a Mine Highwall in Soft Sedimentary Rock. M.Sc. Thesis, University of Alberta.

Small, C.A. and Peterson, A.E., 1988. Monitoring Highwall Deformations. Proceedings Canadian Society for Civil Engineering Annual Conference, Calgary. pp 15-34.

Tsui, P.C. 1988. Geotechnical Investigations of Glaciotectonic Deformation in Central and Southern Alberta. Ph.D. Thesis, University of Alberta, Edmonton, Alberta, Canada.

Varnes, D.J. 1978. Slope Movement and Types and Processes. From Landslides: Analysis and Control. Transportation Research Board, National Agency of Sciences, Washington, D.C. Special Report 176, pp. 11-33.

Wade, N.H. and Peterson, T.W.P., 1986. Highwall monitoring, instrumentation, and stability analysis at the Highvale coal mine, Alberta. International Symposium on Geotechnical Stability in Surface Mining, Calgary, Alberta. pp 373-384.

Figures

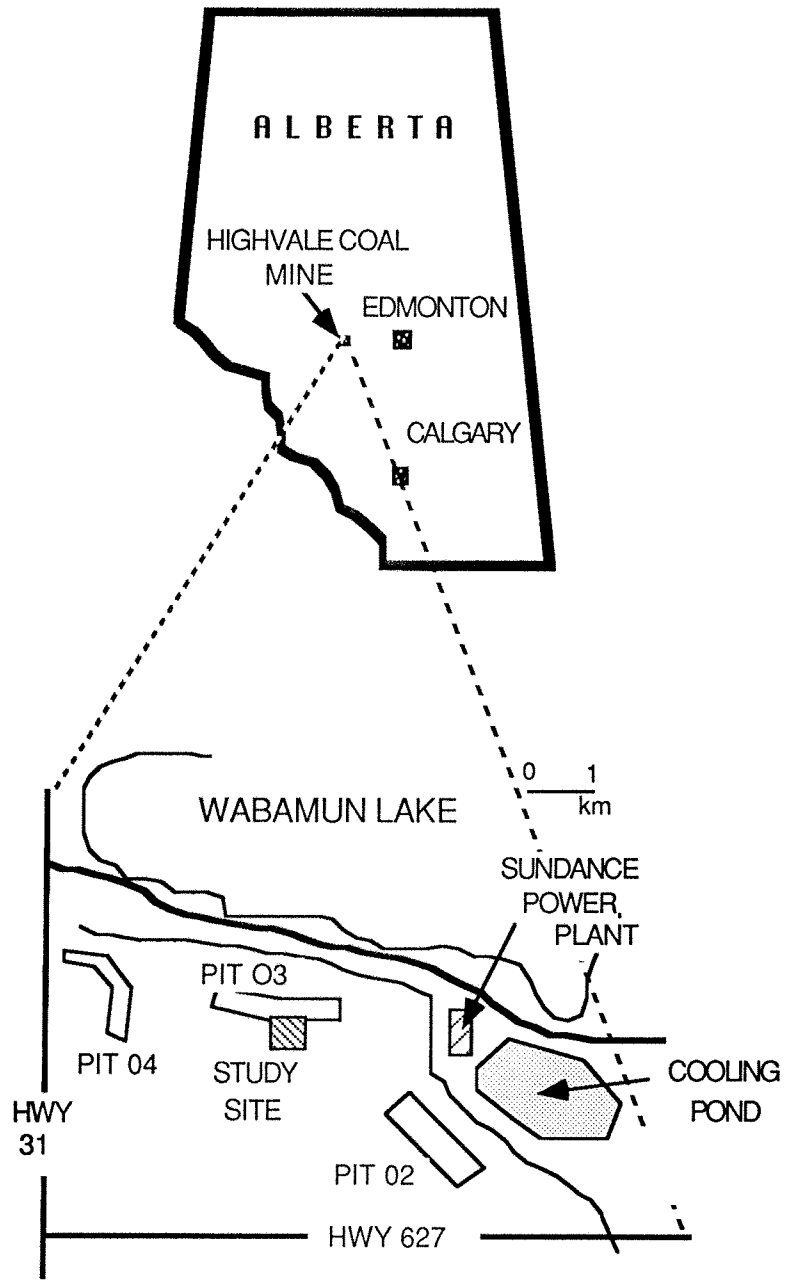

Figure 1. Location of study site at Highvale Coal Mine

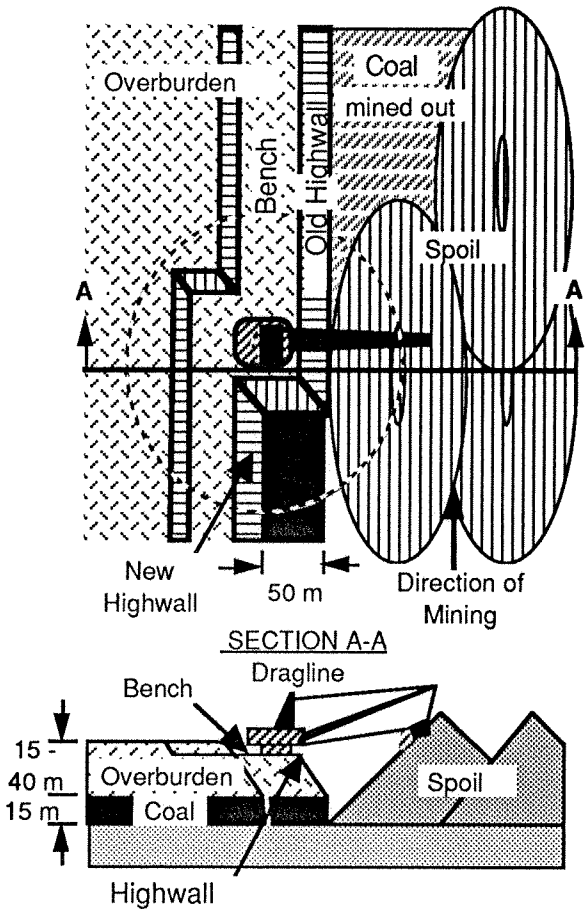

Figure 2. Schematic of mining method at the Highvale Coal Mine

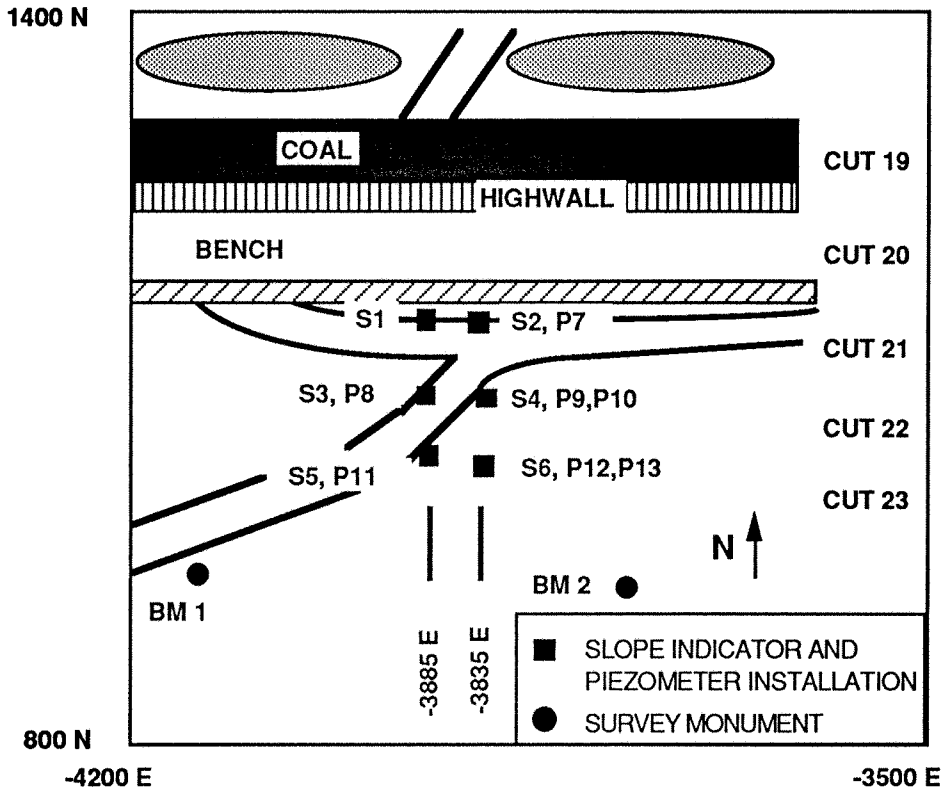

Figure 3. Plan view of study site, June, 1987

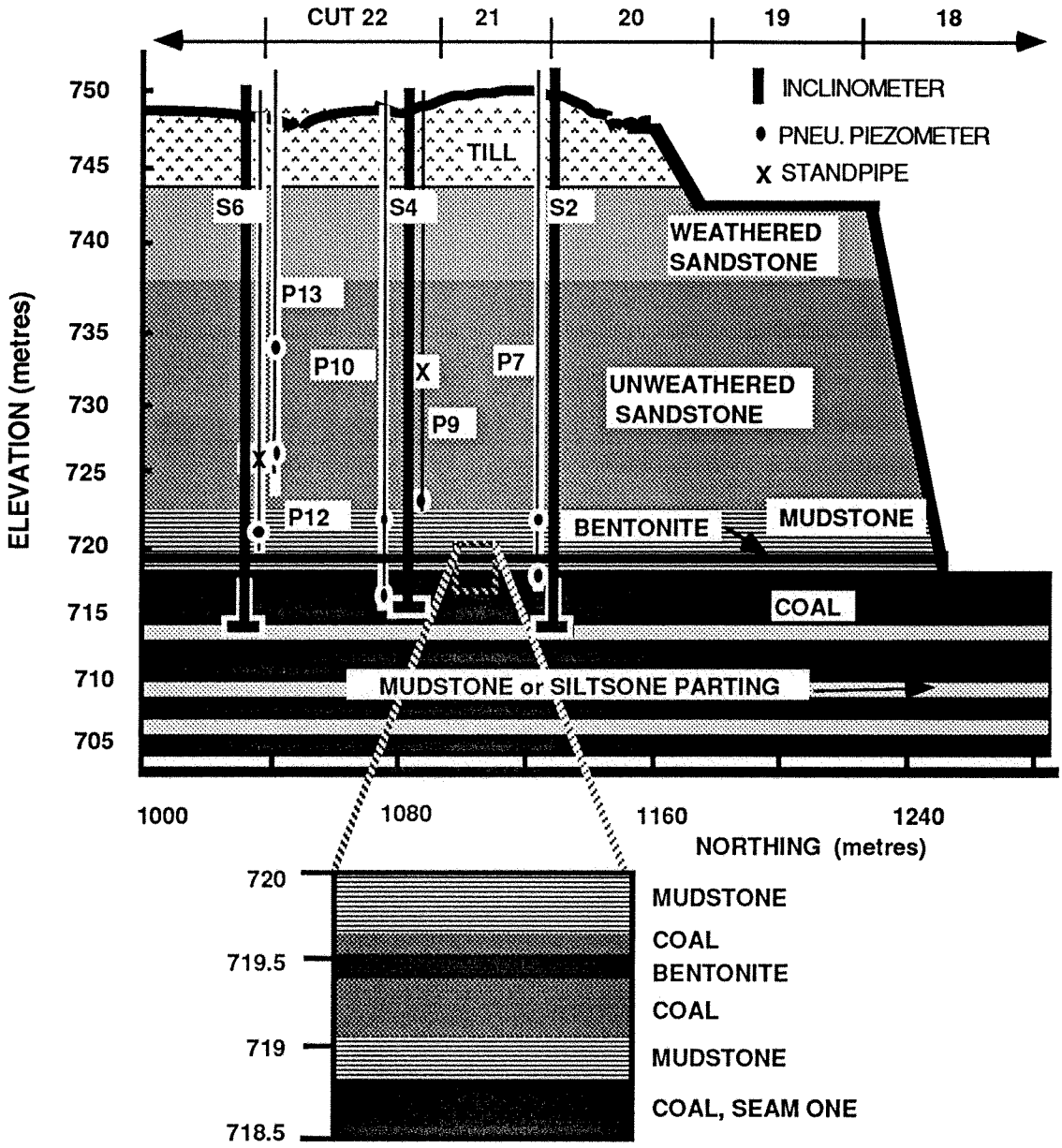

Figure 4. Cross section at study site, Station 3835, Line S2-S4-S6, June, 1987

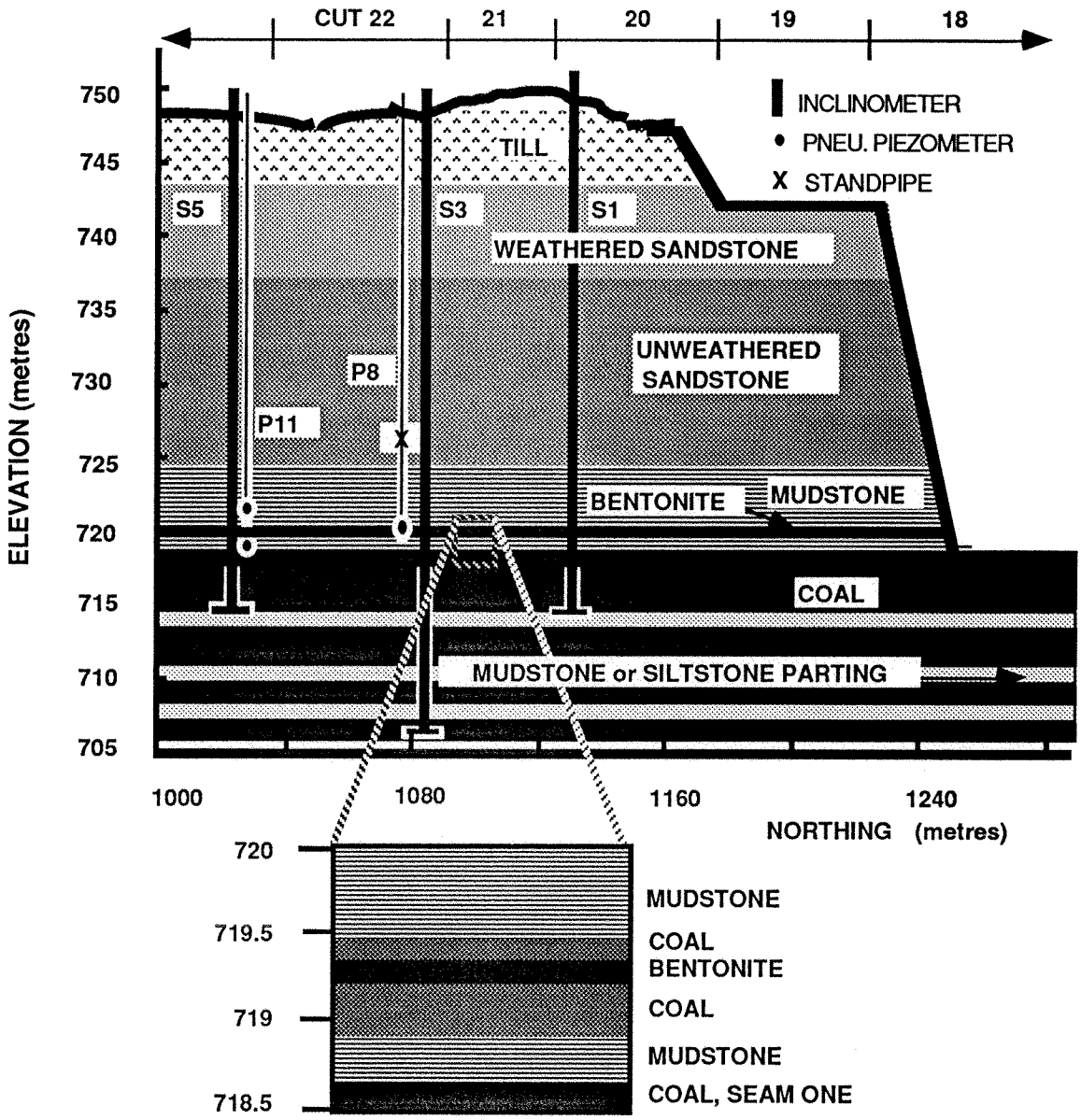

Figure 5. Cross section at study site, Station 3885, Line S1-S3-S5, June, 1987

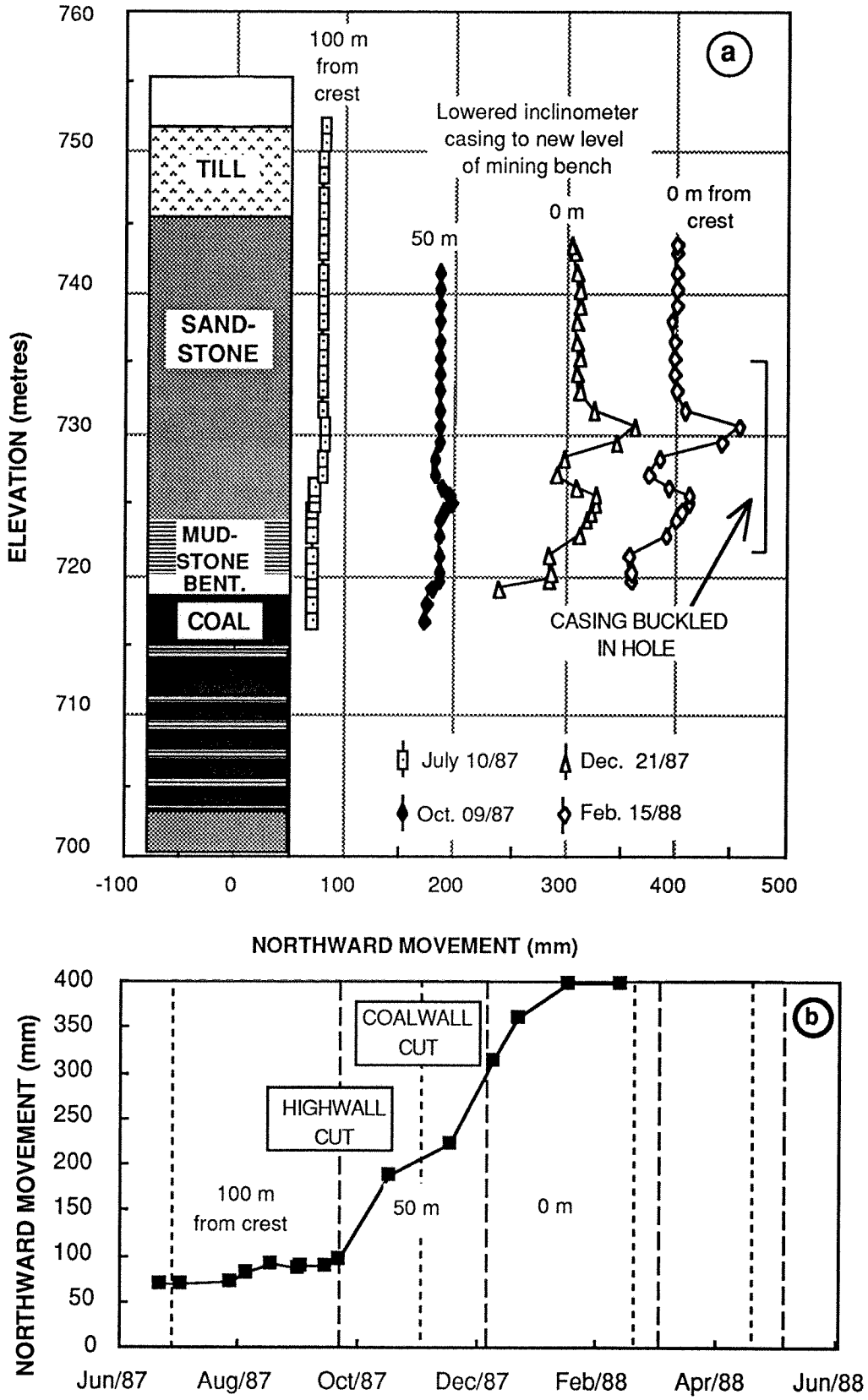

Figure 6. Movement of inclinometer S2. (a) Cumulative deflection profile. (b) Northward movement over time at elevation 730 metres.

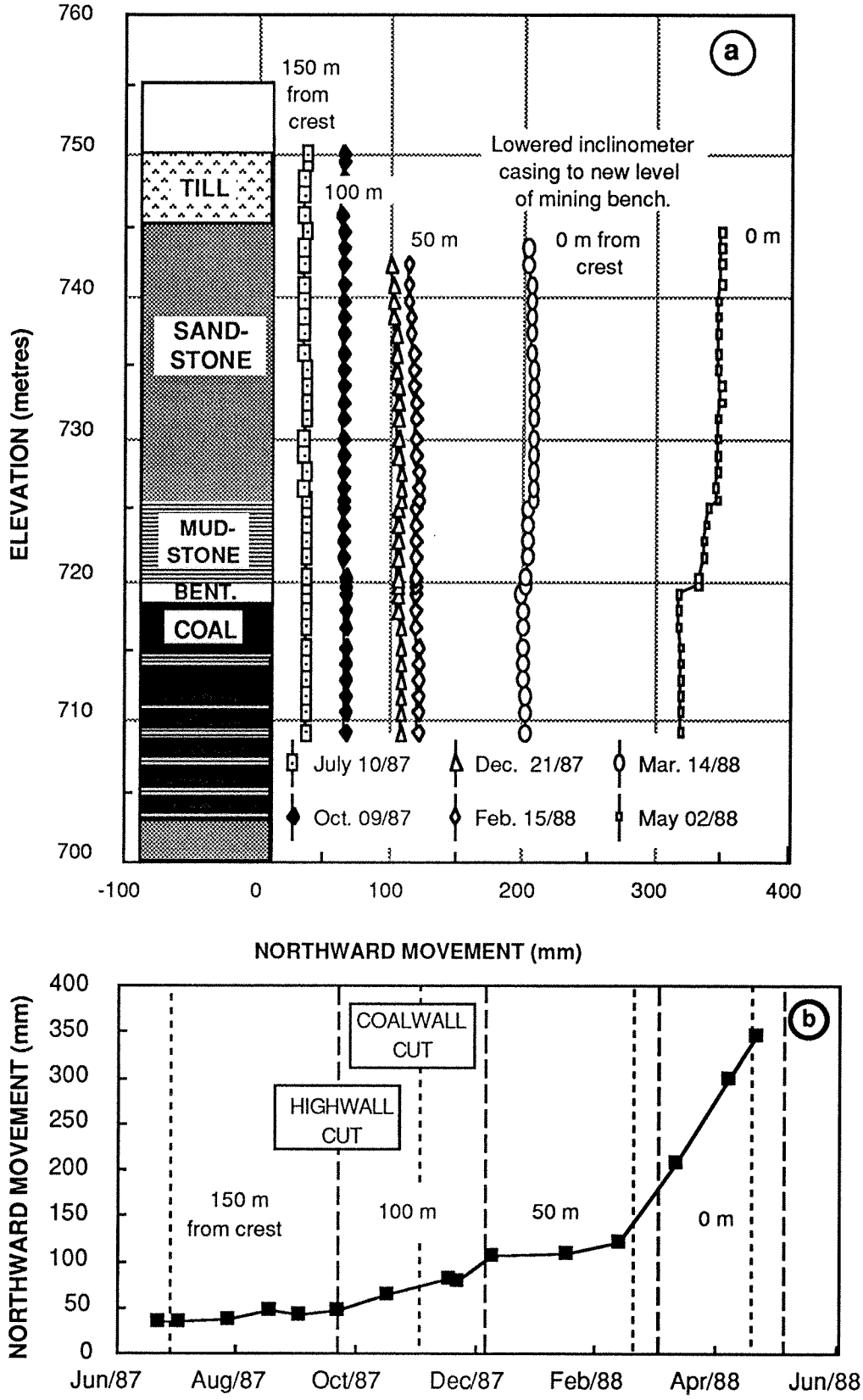

Figure 7. Movement of inclinometer S3. (a) Cumulative deflection profile. (b) Northward movement over time at elevation 730 metres.

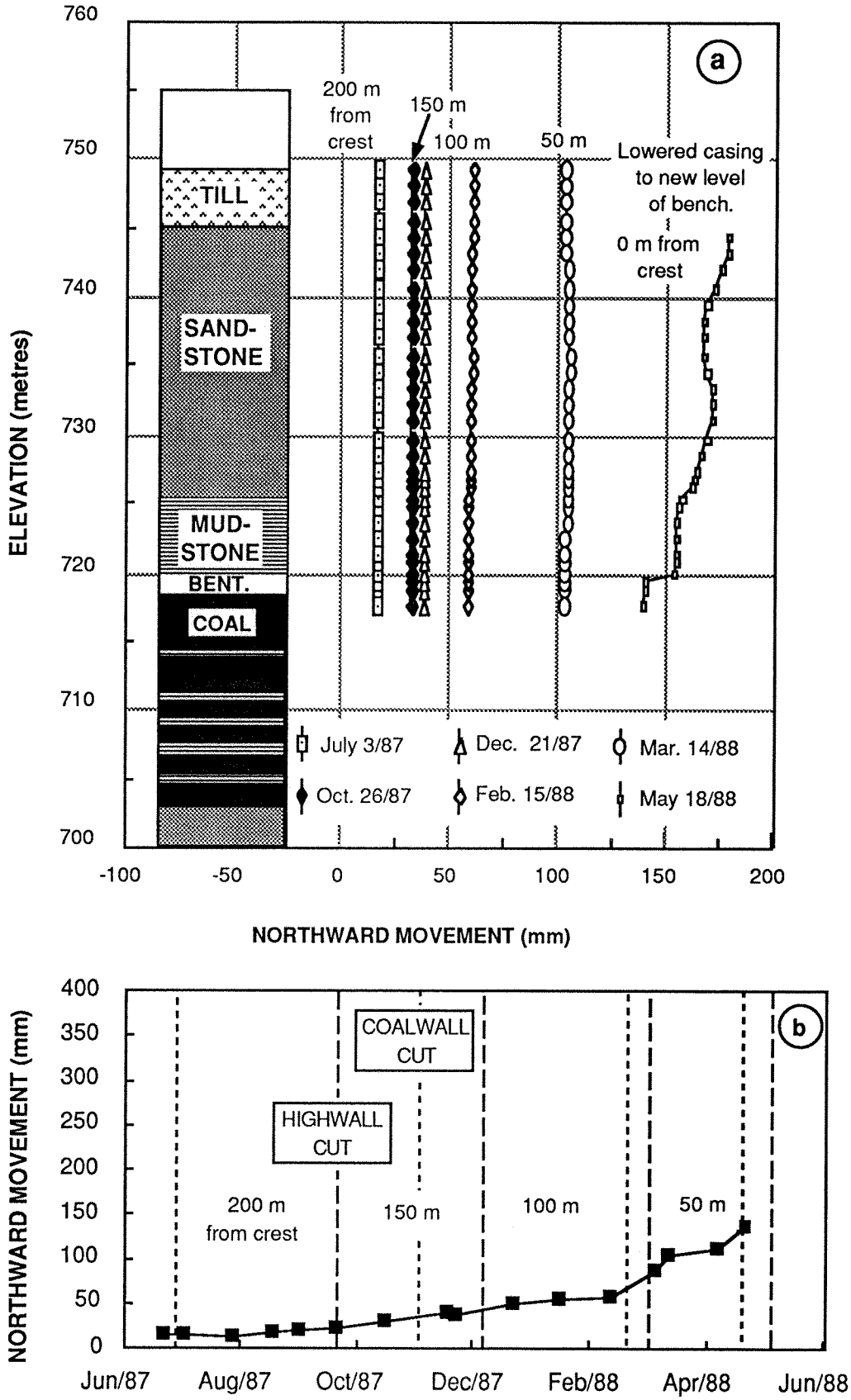

Figure 8. Movement of inclinometer S5. (a) Cumulative deflection profile. (b) Northward movement over time at elevation 730 metres.

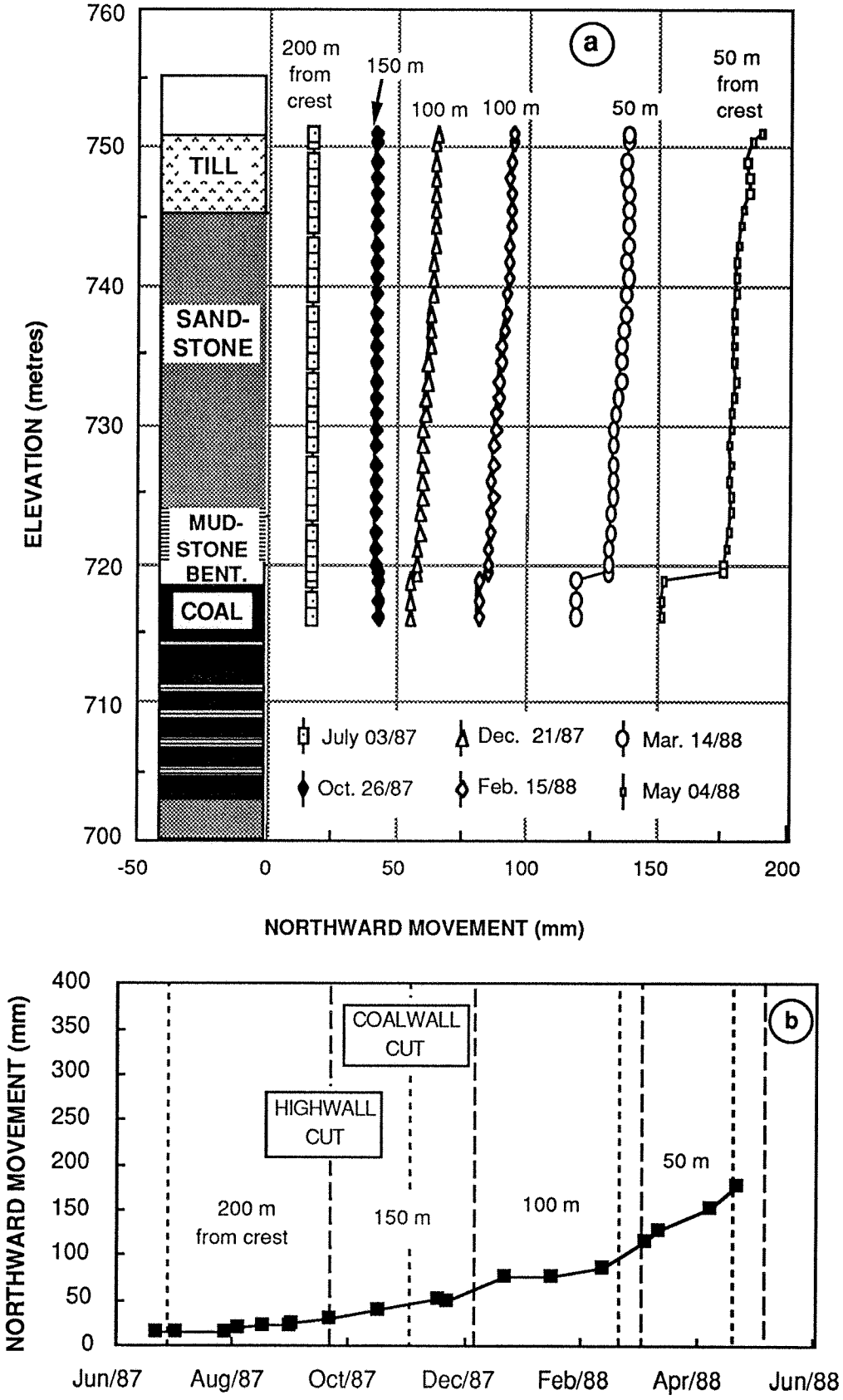

Figure 9. Movement of inclinometer S6. (a) Cumulative deflection profile. (b) Northward movement over time at elevation 730 metres.

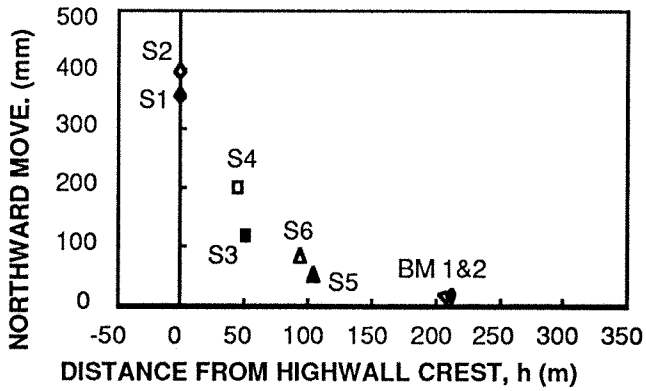

Figure 10. Deformations at elevation 730 metres on February 15, 1988.

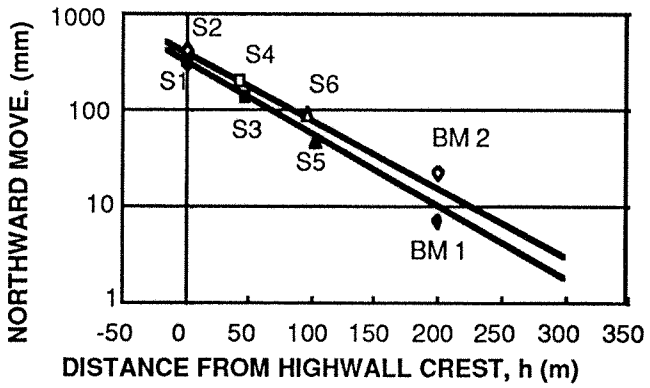

Figure 11. Semi-logarithmic plot of deformations at elevation 730 metres on February 15, 1988.

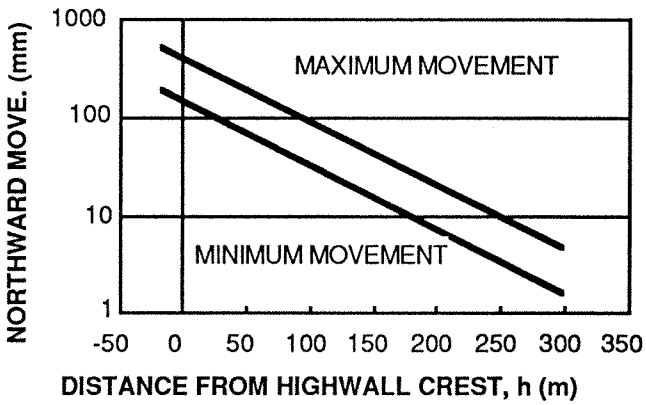

Figure 12. Range of movements measured in the overburden at elevation 730 metres.

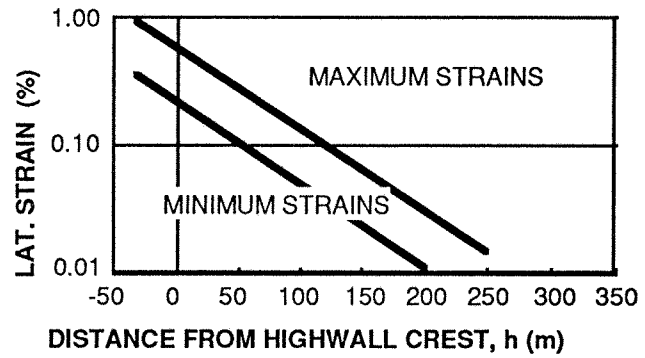

Figure 13. Range of lateral (extension) strains measured in the overburden at elevation 730 metres.

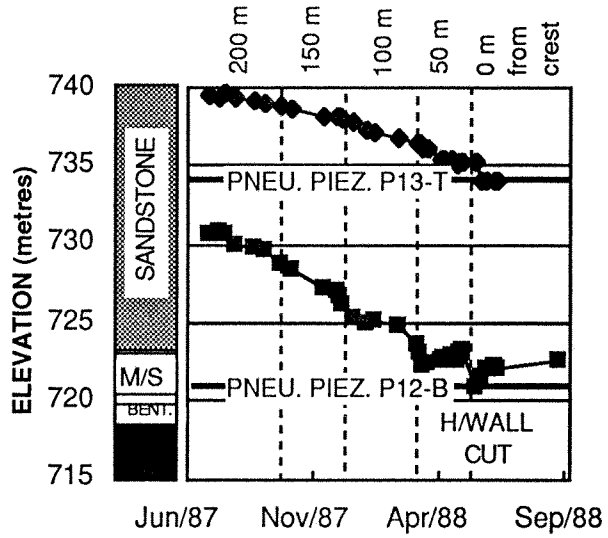

Figure 14. Piezometric head over time at piezometers P12-B and P13-T.

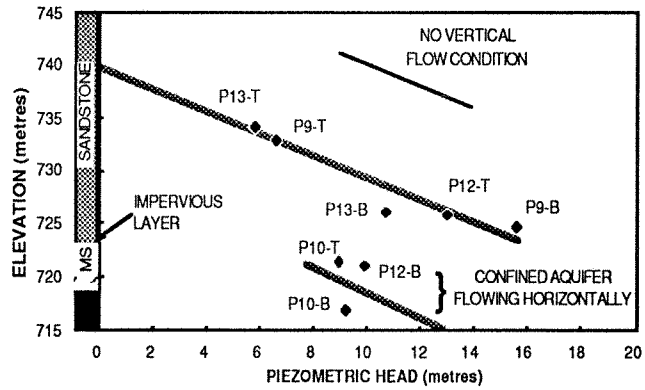

Figure 15. Distribution of piezometric head for piezometers located 200 metres south of the highwall crest.

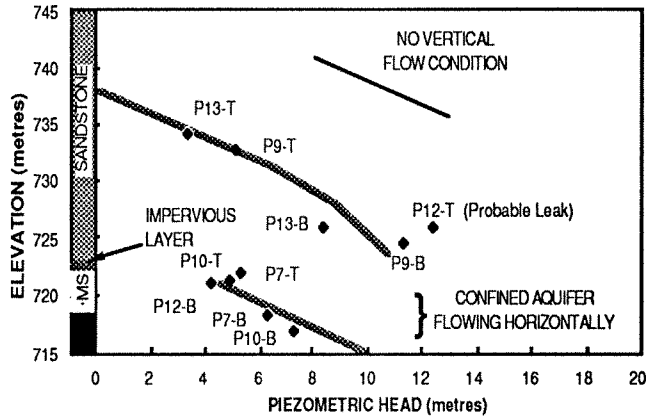

Figure 16. Distribution of piezometric head for piezometers located 100 metres south of the highwall crest.

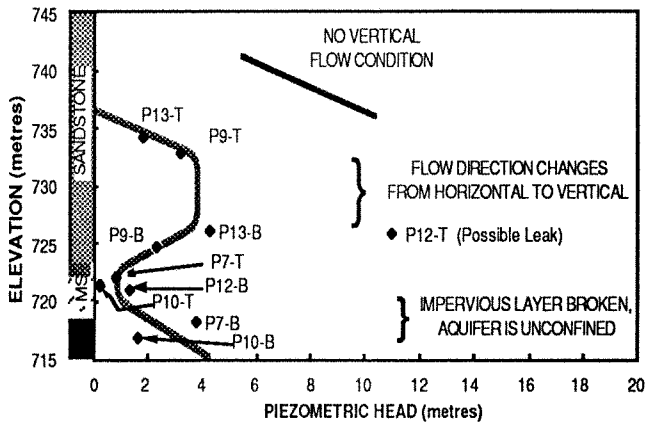

Figure 17. Distribution of piezometric head for piezometers located 50 metres south of the highwall crest.

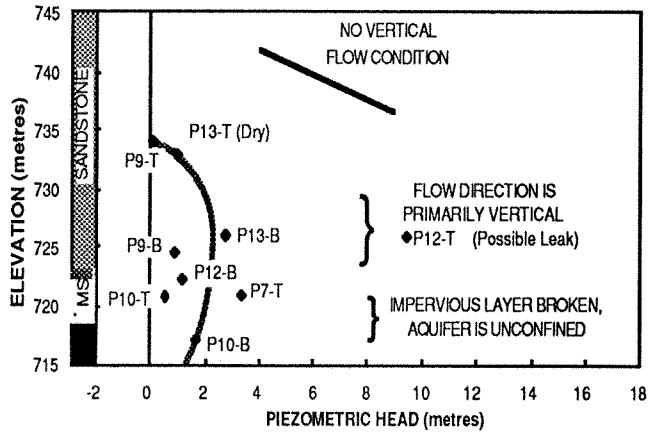

Figure 18. Distribution of piezometric head for piezometers located beneath the highwall crest. Three to four weeks after a highwall was cut.

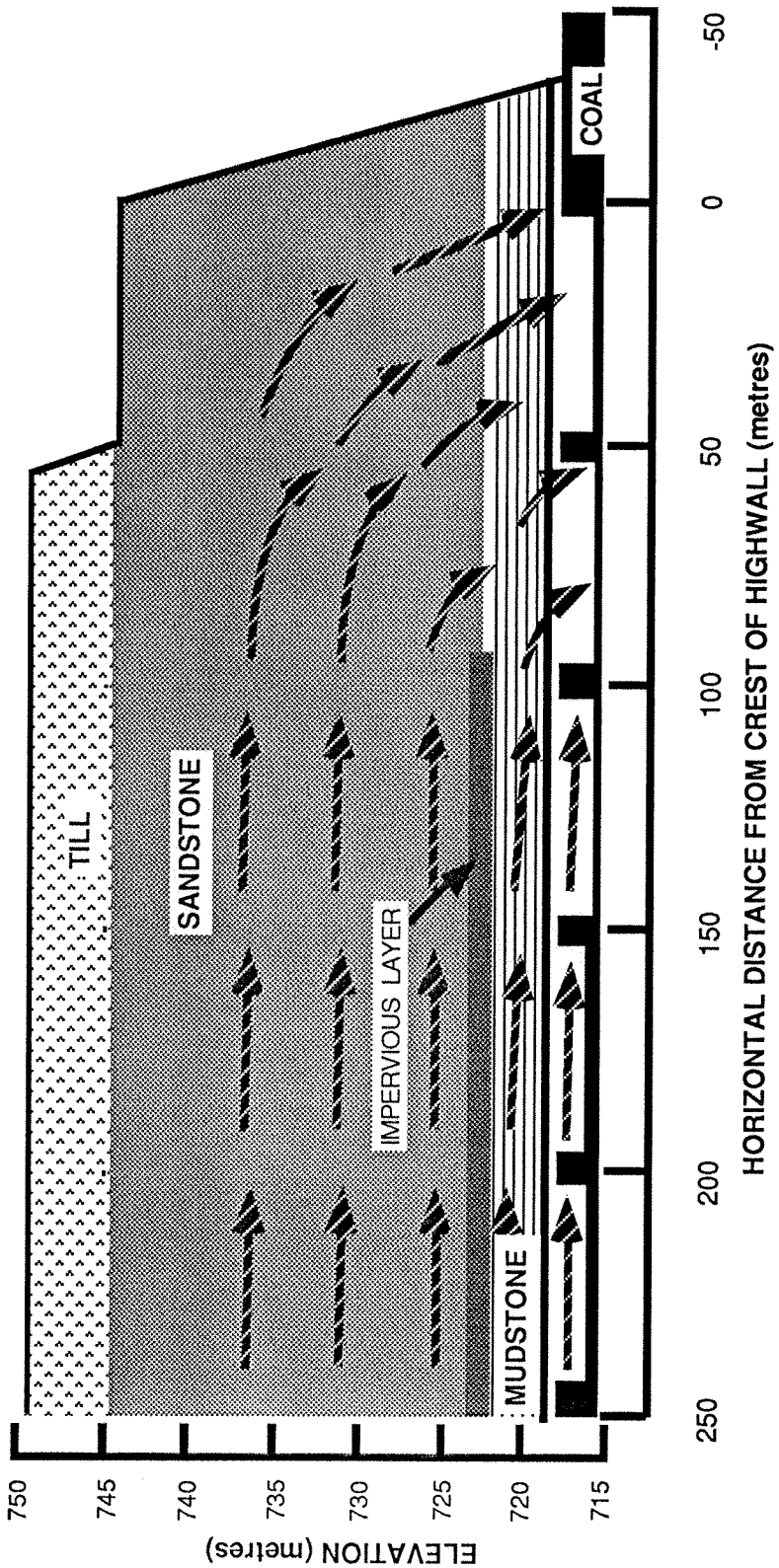

Figure 19. Schematic of groundwater flow pattern in overburden.

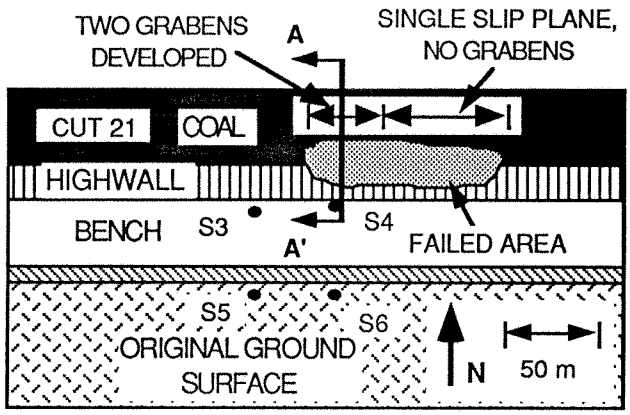

Figure 20. Plan view of failure in highwall Pit 03, April, 1988.

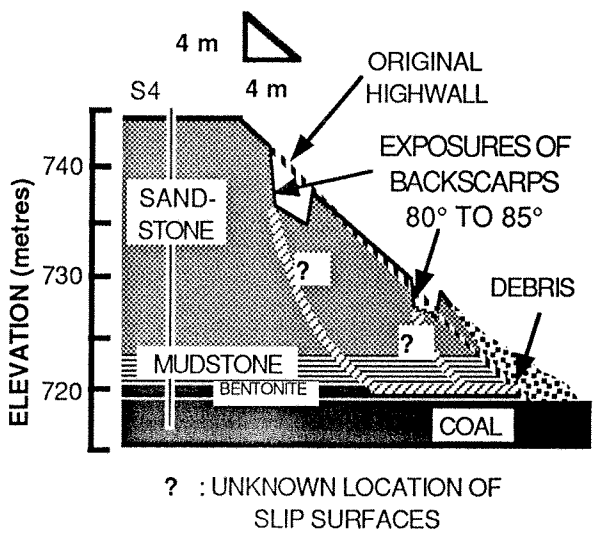

Figure 21. Post failure topography at Section A-A' through west end of failure, as observed on April 7, 1988.

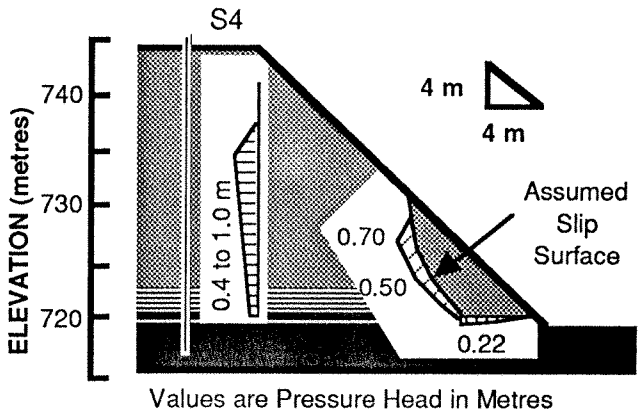

Figure 22. Pore pressure distribution assumed for back analysis of toe failure.

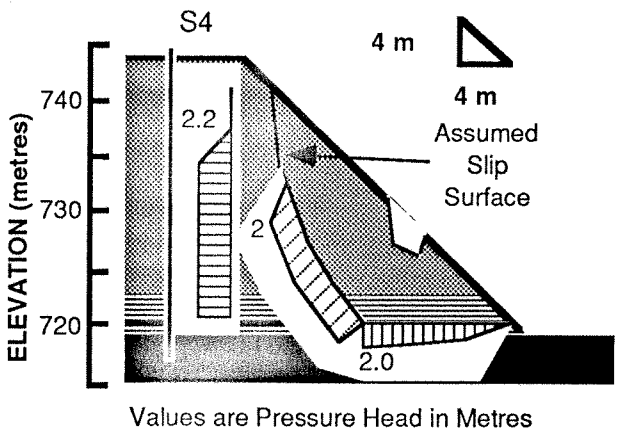

Figure 23. Pore pressure distribution assumed for back analysis of rear failure. Toe had previously failed.

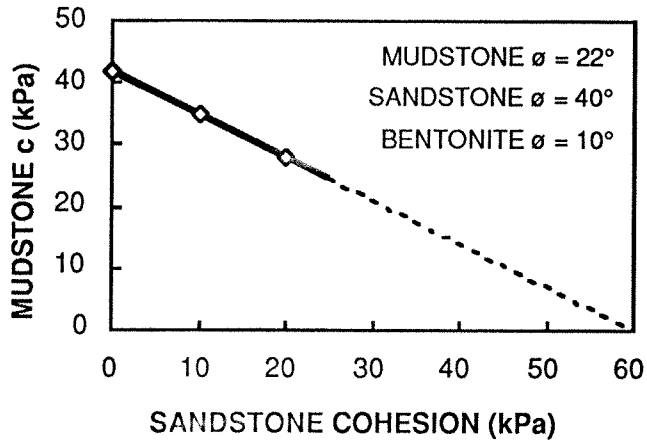

Figure 24. Combinations of mudstone and sandstone cohesions mobilized at toe failure.

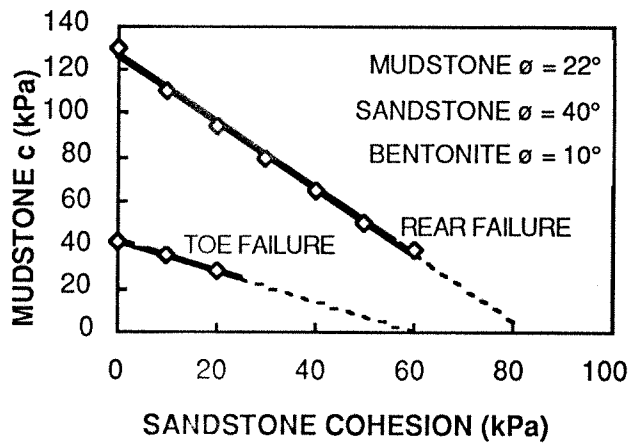

Figure 25. Combination of mudstone and sandstone cohesions mobilized at toe and rear failures.